Proceedings of the 45th IEEE Conference on Decision & Control
Manchester Grand Hyatt Hotel
San Diego, CA, USA, December 13-15, 2006

WeIP3.7

2H Singularity-Free Momentum Generation with

Non-Redundant Single Gimbaled Control Moment Gyroscopes

Timothy A. Sands, Jae Jun Kim, Brij Agrawal

Abstract—Two objectives dominate consideration of control moment gyroscopes (CMGs) for spacecraft maneuvers: High torque (equivalently momentum) and singularity-free operations. This paper adds to the significant body of research towards these two goals utilizing a minimal 3-CMG array to provide 646% singularity-free momentum performance increase *spherically*, compared to the ubiquitous pyramid arrangement skewed at 54.73°. Spherical 1H (1 CMGs-worth momentum) *singularity free* momentum is established with birectional 1H and 2H in the third direction in a baseline configuration. Lastly, momentum space reshaping is shown via mixed skew angles. These claims are demonstrated analytically, then heuristically, and finally validated experimentally.

I. INTRODUCTION

Rapid spacecraft reorientation often drives design engineers to consider Control Moment Gyroscopes (CMGs). CMGs are momentum exchange devices that exhibit extreme torque magnification (i.e. for a small amount of torque input to the CMG gimbal motors, a large resultant output torque is achieved).
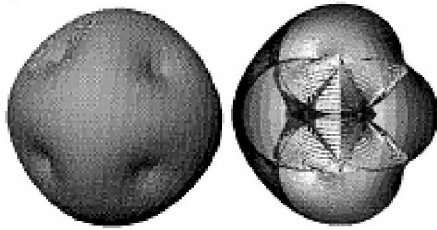

Fig. 1. Left: External (4H & 0H) singularity surfaces typically used to define the "optimal spherical" skew angle, ß=54.73° . Right: Internal (1H & 2H) singularities generate errors & potential instability as momentum trajectory strikes one of these surfaces. [2]

Typical CMG's output torques are on the order of hundreds to thousands of times the torque output of reaction wheels, another kind of momentum exchange attitude control actuator. A unique challenge of CMG implementation is mathematical singularity. Arguably, the most common configuration for a skewed array of 4 CMGs is the "pyramid" array where the 4 CMGs are skewed at an angle of β=54.73° resulting in an "optimal spherical" momentum capability [1] requiring internal singularity avoidance [3]-[9]. The desire is often stated as an equivalent, *maximized* momentum capability in all directions based on the {++++} or {----} 0H & 4H saturation singularities where all four CMGs are pointing in the same direction (Fig. 5). The typical design approach may be succinctly stated: 1) Optimize spherical momentum, then 2) minimize impact of singularities. The approach adopted here will reverse the traditional approach as follows: 1) Minimize singularities, and then 2) maximize spherical momentum. Surprisingly, the result turns out quite differently.

II. TORQUE GENERATION AND SINGULARITIES

To achieve a specified output torque from a CMG array, a command must be sent to the gimbal motor. Eqn. (1) shows this relationship for i=n CMGs normalized by one CMG's worth of momentum ($1H$). CMGs are inclined so gimbal planes form skew angles, $ß_i$ with respect to the xy plane as depicted in Fig. 2. The [**A**] matrix (containing gimbal angles, $θ_i$ and skew angles, $ß_i$) must be inverted to find the required CMG gimbal command for commanded output torque per equation (2). Begin by writing equations for each momentum vector in xyz coordinates for 3 CMGs normalized by 1H.

$$\left.\begin{aligned} \mathbf{h_x} &= \cos\theta_3 - \cos\theta_1 + \cos\beta\sin\theta_2 \\ \mathbf{h_y} &= \cos\beta(\sin\theta_3 - \sin\theta_1) - \cos\theta_2 \\ \mathbf{h_z} &= \cos\beta(\sin\theta_1 + \sin\theta_2 + \sin\theta_3) \end{aligned}\right\} \mathbf{H} = \mathbf{h_x}\hat{\mathbf{x}} + \mathbf{h_y}\hat{\mathbf{y}} + \mathbf{h_z}\hat{\mathbf{z}}$$

$$\frac{\partial \mathbf{H}}{\partial\theta} = \left\{\begin{matrix} \partial\mathbf{h_x}/\partial\theta_i \\ \partial\mathbf{h_y}/\partial\theta_i \\ \partial\mathbf{h_z}/\partial\theta_i \end{matrix}\right\} = \underbrace{\begin{bmatrix} \sin\theta_1 & \cos\beta\cos\theta_2 & -\sin\theta_3 \\ -\cos\beta\cos\theta_1 & \sin\theta_2 & \cos\beta\cos\theta_3 \\ \sin\beta\cos\theta_1 & \sin\beta\cos\theta_2 & \sin\beta\cos\theta_3 \end{bmatrix}}_{[\mathbf{A}]}$$

		Form Approved
	Report Documentation Page	*Form Approved* *OMB No. 0704-0188*

Public reporting burden for the collection of information is estimated to average 1 hour per response, including the time for reviewing instructions, searching existing data sources, gathering and maintaining the data needed, and completing and reviewing the collection of information. Send comments regarding this burden estimate or any other aspect of this collection of information, including suggestions for reducing this burden, to Washington Headquarters Services, Directorate for Information Operations and Reports, 1215 Jefferson Davis Highway, Suite 1204, Arlington VA 22202-4302. Respondents should be aware that notwithstanding any other provision of law, no person shall be subject to a penalty for failing to comply with a collection of information if it does not display a currently valid OMB control number.

1. REPORT DATE **DEC 2006**	2. REPORT TYPE	3. DATES COVERED **00-00-2006 to 00-00-2006**
4. TITLE AND SUBTITLE **2H Singularity-Free Momentum Generation with Non-Redundant Single Gimbaled Control Moment Gyroscopes**		5a. CONTRACT NUMBER
		5b. GRANT NUMBER
		5c. PROGRAM ELEMENT NUMBER
6. AUTHOR(S)		5d. PROJECT NUMBER
		5e. TASK NUMBER
		5f. WORK UNIT NUMBER
7. PERFORMING ORGANIZATION NAME(S) AND ADDRESS(ES) **Naval Postgraduate School,Monterey,CA,93943**		8. PERFORMING ORGANIZATION REPORT NUMBER
9. SPONSORING/MONITORING AGENCY NAME(S) AND ADDRESS(ES)		10. SPONSOR/MONITOR'S ACRONYM(S)
		11. SPONSOR/MONITOR'S REPORT NUMBER(S)

12. DISTRIBUTION/AVAILABILITY STATEMENT **Approved for public release; distribution unlimited**

13. SUPPLEMENTARY NOTES

14. ABSTRACT

Abstract-Two objectives dominate consideration of control moment gyroscopes (CMGs) for spacecraft maneuvers: High torque (equivalently momentum) and singularity-free operations. This paper adds to the significant body of research towards these two goals utilizing a minimal 3-CMG array to provide 646% singularity-free momentum performance increase spherically, compared to the ubiquitous pyramid arrangement skewed at 54.730. Spherical 1H (1 CMGs-worth momentum) singularity free momentum is established with birectional 1H and 2H in the third direction in a baseline configuration. Lastly, momentum space reshaping is shown via mixed skew angles. These claims are demonstrated analytically, then heuristically, and finally validated experimentally.

15. SUBJECT TERMS					
16. SECURITY CLASSIFICATION OF:			17. LIMITATION OF ABSTRACT	18. NUMBER OF PAGES	19a. NAME OF RESPONSIBLE PERSON
a. REPORT **unclassified**	b. ABSTRACT **unclassified**	c. THIS PAGE **unclassified**	**Same as Report (SAR)**	**6**	

Standard Form 298 (Rev. 8-98)
Prescribed by ANSI Std Z39-18

The Newton-Euler relation relates generated torque to the timed-rate of change of angular momentum of the spacecraft system. A CMG absorbs momentum change, $\dot{\mathbf{H}}$ causing an equal and opposite change in momentum on the spacecraft. For n CMGs, the general relation is:

$$\dot{\mathbf{H}} = \frac{\partial \mathbf{H}}{\partial \theta_i}\frac{\partial \theta_i}{\partial t} = \frac{\partial \mathbf{H}}{\partial \theta_i}\dot{\theta} = \sum_{i=1}^{n}\mathbf{h}_i = \sum_{i=1}^{n}\mathbf{a}_i(\theta_i)\dot{\theta}_i = [\mathbf{A}]\{\dot{\theta}\} \quad (1)$$

$$[\mathbf{A}]^{-1}\dot{\mathbf{H}} = [\mathbf{A}]^{-1}[\mathbf{A}]\{\dot{\theta}\} = \{\dot{\theta}\} \quad (2)$$
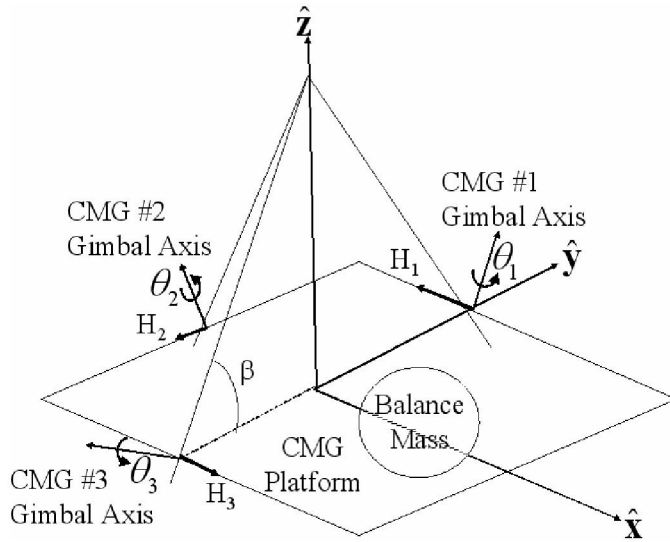

Fig. 2. 3/4 Skewed CMG array utilized in this study

For some combinations of gimbal & skew angles, the [**A**] matrix columns can become linearly dependent. At these combinations of skew and gimbal angles, the determinant of the [**A**] matrix becomes zero leading to singular inversion.

$$\det[\mathbf{A}] = s\beta\left\{s\theta_2\left[s(\theta_1+\theta_3)\right] + c\beta c\theta_2\left[s(\theta_3-\theta_1)+2c\theta_1 c\theta_3 c\beta\right]\right\}$$
$$\text{where } s = \sin, \ c = \cos$$

III. THE 3/4 SKEWED CMG ARRAY

The 3/4 CMG array modifies the commonly studied 4 CMG skewed pyramid. A minimum of 3 CMGs is required for 3-axis control, and the fourth it often used for singularity avoidance. With the 3/4-array, only 3 CMGs are utilized for active attitude control with the fourth CMG held in reserve for robust failure properties. Experimental verification will be provided in later sections utilizing a spacecraft testbed with a 3/4 CMG array containing a balance mass in the place of the fourth CMG (Fig. 2).

The approach taken by the author is to first optimize the 3/4 skewed array geometry itself by choosing the skew angle that provides the greatest singularity-free momentum. At this "optimal *singularity-free*" skew angle, the 3/4 CMG array can operate at momentum values less than the singularity-free threshold without any kind of singularity avoidance

scheme. Further, utilization of mixed skew angles can rotate the workspace to maximize momentum in a preferred direction, again singularity-free. Yaw is the preferred direction in this study. A direct comparison with the traditional "optimal spherical" skew angle will demonstrate the dramatic improvement in torque capability of the CMG array. Analytical derivation is followed by heuristic, geometric analysis, then validation via experimentation on a realistic spacecraft simulator in ground tests.

IV. ANALYTICAL ANALYSIS

Singular combinations of gimbal angles and skew angles can be determined analytically by examining the determinant of the [**A**] matrix. When the determinant goes to zero, the matrix has linearly dependent columns resulting in singular inversion. There are six cases (with multiple sub-cases) that result in a singular [**A**] matrix (less than full rank) with $\beta_i = \beta$.

Case 1:
$$\sin\beta^0\left\{\sin\theta_2\left[\sin(\theta_1+\theta_3)\right] + \cos\beta\cos\theta_2\left[\sin(\theta_3-\theta_1)+2\cos\theta_1\cos\theta_3\cos\beta\right]\right\}$$

Case 2:
$$\sin\beta\left\{\sin\theta_2\left[\sin(\theta_1+\theta_3)\right]^0 + \cos\beta\cos\theta_2\left[\sin(\theta_3-\theta_1)\pm2\cos\theta_1\cos\theta_3\cos\beta\right]^0\right\}$$

Case 3:
$$\sin\beta\left\{\sin\theta_2\left[\sin(\theta_1+\theta_3)\right] + \cos\beta\cos\theta_2\left[\sin(\theta_3-\theta_1)+2\cos\theta_1\cos\theta_3\cos\beta\right]^0\right\}$$

Case 4:
$$\sin\beta\left\{\sin\theta_2^{-0}\left[\sin(\theta_1+\theta_3)\right] + \cos\beta\cos\theta_2^{-0}\left[\sin(\theta_3-\theta_1)+2\cos\theta_1\cos\theta_3\cos\beta\right]\right\}$$

Case 5:
$$\sin\beta\left\{\sin\theta_2\left[\sin(\theta_1+\theta_3)\right]^0 + \cos\beta\cos\theta_2^{-0}\left[\sin(\theta_3-\theta_1)+2\cos\theta_1\cos\theta_3\cos\beta\right]\right\}$$

Case 6:
$$\sin\beta\left\{\sin\theta_2^{-0}\left[\sin(\theta_1+\theta_3)\right] + \cos\beta\cos\theta_2\left[\sin(\theta_2-\theta_1)\pm2\cos\theta_1\cos\theta_3\cos\beta\right]^0\right\}$$

There are a few trivial cases. Nontrivial cases may be analyzed as follows. In general, for a given skew angle, each case produces gimbal angle combinations that result in $\det[\mathbf{A}]=0$. These gimbal combinations may be used to calculate the resultant momentum at the singular condition $|\mathbf{H}|_{minSingular}$. Minimum singular momentum values may then be plotted for iterated skew angles $0° < \beta < 90°$. Having established the minimum value of momentum at singular combinations of gimbal angles, it is not possible to become singular at momentum less that these values (Fig. 3). Thus the result is the maximum singularity-free momentum space, Fig. 7.

V. HEURISTIC ANALYSIS

The preceding analysis reveals singularity free operations <1H in all directions by implication. While useful, the analysis certainly does not yield much intuition for the attitude control engineer to design safe momentum trajectories through the momentum space. Are there directions that can exceed 1H singularity-free?
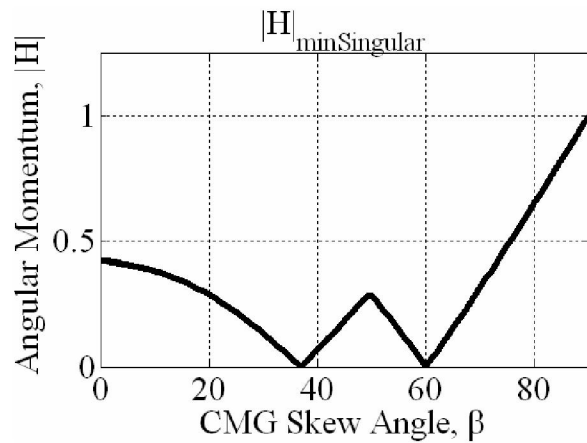
1552

Fig. 3. Skew angle optimization for maximum singularity-free normalized momentum
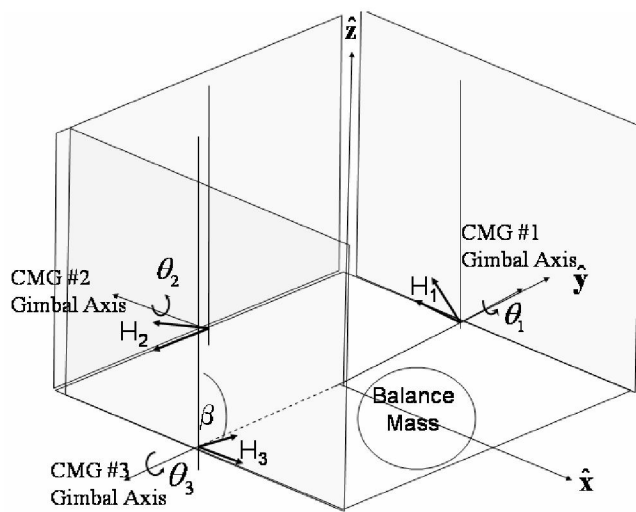

Fig. 4. 3/4 CMG skewed array momentum cutting planes with ß=90°.

Recent advances in computer processors speeds make a heuristic approach quickly accomplished. Consider rotating a vector $360°$ creating a CMG gimbal "cutting" plane (discretized at some interval). Then rotate the gimbal plane $360°$ creating a lattice of discrete points forming a solid, filled sphere. This lattice provides discretized points to analyze CMG array momentum. This is easily done in embedded loops of computer code. Each discrete point corresponds to a set of three coordinates or equivalently three gimbal angles. At each discrete point, singularity/non-singularity of [**A**] is established. *At singular points*, the normalized magnitude of angular momentum may be calculated. A point may be plotted at the magnitude of the momentum in the singular direction. This results in a three dimensional singularity map granting *easy* intuition for maneuvering in the momentum space. Singular surfaces result from several kinds of singularities: 0H, 1H, 2H, and 3H depicted in Fig. 5. Typically, the "optimal spherical" skew angle is determined by the outer, saturation singular surface alone (0H & 3H in this case of a 3/4 CMG array). In order to find the maximum *singularity-free* skew angle, the analysis absolutely must

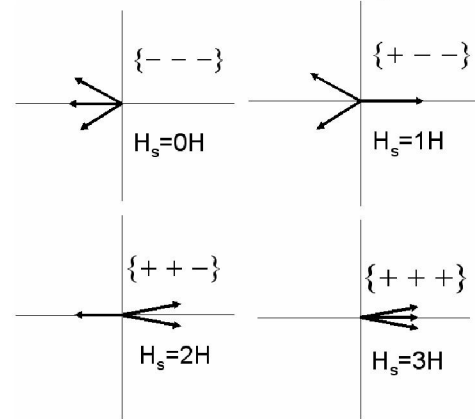also account for the 1H and 2H internal singularities.

Fig. 5. Individual CMG momentum directions for a 3/4 CMG skewed array in a singular configuration of gimbal angles.

It may be noted here that the often used "optimal spherical" skew angle (β=54.73°) that results in equivalent momentum in all directions is derived utilizing the 0H {----} & 4H {++++} singular surface of a 4 CMG skewed array. The 0H & 4H singular surface is the saturation surface that results from all 4 CMGs pointing in the same direction, and it's corresponding saturation surface for the 3/4 array is the 0H & 3H singular surface. In the case of a 3/4 CMG array the singular surfaces are depicted in Fig. 6 for the often used "optimal spherical" momentum skew angle (β=54.73°).
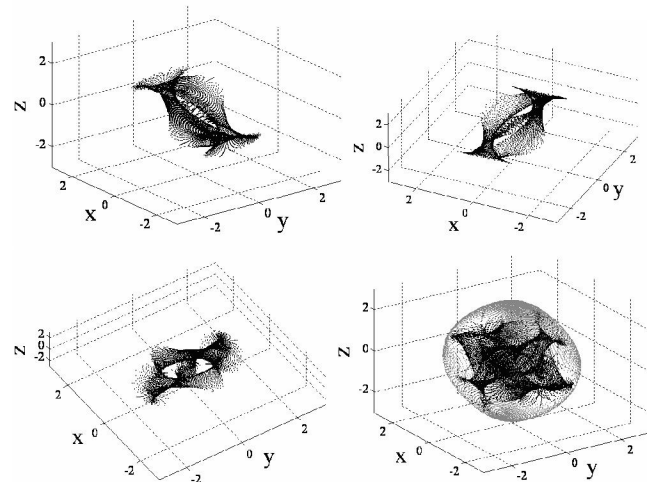

Fig. 6. Singular surfaces for 3/4 CMG skewed array at "optimal spherical " momentum skew angle ß=54.73° . Top: 1H & 2H surfaces, Bottom left: 1H & 2H surface; Bottom right=1H & 2H surfaces inside 0H & 3H surfaces.

Note the spherical nature of the external, saturation singular surface {+++} & {---} typified by the ubiquitous 4 CMG pyramid array skewed at β=54.73° is nearly maintained in the 3/4 array. The internal 1H and 2H singularities are quite a problem, since they occupy a large portion of the momentum space. The combined singularity hypersurface makes it difficult to see a clear momentum path away from the origin (0,0,0). This is quite important, since CMGs must spin

1553

up at a zero-momentum gimbal angle configuration lest they impart massive torques onto the spacecraft. $\{\theta_1, \theta_2, \theta_3\}=\{0,0,0\}$ is one very common zero-momentum spin-up configuration.
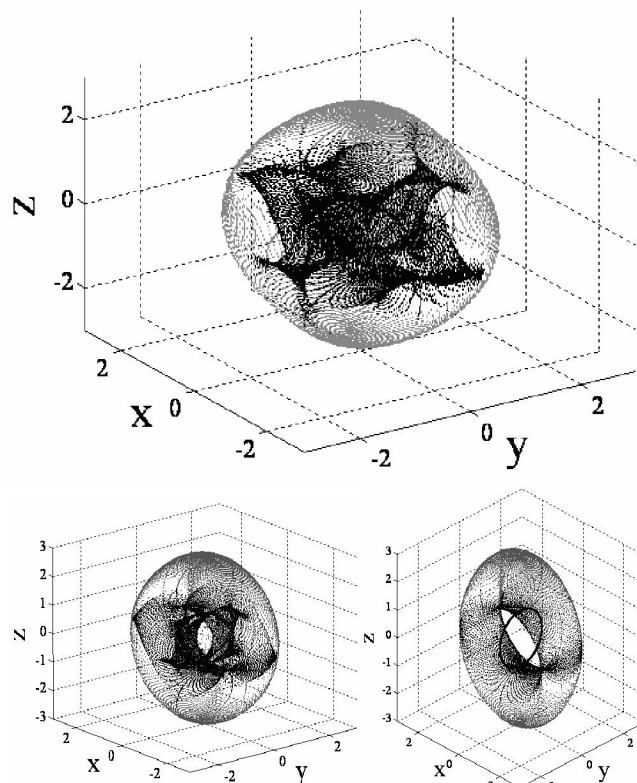

Fig. 7. Heuristic analysis varying skew angle, β for a 3/4 CMG skewed array. β was varied in 5° increments from 0° to 90° identifying the trend represented here by three primary plots with 3H &0H singular surface lightened to enable visualization of 1H & 2H singular surfaces: $\beta=70^\circ$ (top), 80° (lower left), 90° (lower right).

The typical design methodology might use the shape of the 3H outer momentum surface {+++} & {---} to define $\beta=54.73$ as the "optimal spherical" momentum skew angle. The attitude control engineer would be left with the daunting task of maneuvering in this crowded momentum space while trying to avoid any point on the singular hypersurface. Striking a singular point results in (at least temporary) loss of attitude control.   Also note the maximum momentum capability is less than 3H.   Per Fig. 3, the maximum *singularity-free* momentum capability using $\beta=54.73^\circ$ is 0.154868. If the skew angle were increased to ninety degrees, *singularity-free* momentum would be increased 646% to 1.0. Consider the singular hypersurfaces for heuristic, geometric observations.

It was established in sections IV that a skew angle of ninety degrees results in a singularity-free momentum space of 1H for the 3/4 CMG array.   Repeating the numerical, heuristic singularity analysis as skew angle increases is very revealing. Fig. 7 displays the singular momentum space for a skew angle of 70°, then 80°, then 90°. Notice how the 1H & 2H singular surfaces move away from the (0,0,0) momentum

point and gradually converge into each other as skew angle increases to ninety degrees. Fewer singular surfaces is obviously beneficial, but the vacancy of the center of the momentum space is marvelous. Furthermore, the singularity-free momentum space can be rotated via mixed skew angles to emphasize a preferred axis of rotation.

VI.   MIXED SKEW ANGLES

Typically, skewed CMG arrays utilize identical skew angles for each CMG ($\beta_i=\beta$). By using mixed skew angles, the singularity-free "football" shaped space can be reoriented to place the maximum momentum direction in the yaw direction. Six possible momentum reorientations are possible by laying down momentum planes from ninety degrees to zero degrees as listed in Fig. 8 resulting in rotations of the momentum space depicted respectively in Fig. 9.

β_1	β_2	β_3
0°	90°	90°
90°	0°	90°
90°	90°	0°
0°	0°	90°
0°	90°	0°
90°	0°	0°

Fig. 8. Six possible combinations of mixed skew angles laying one or two momentum cutting planes from 0° to 90°. Corresponding singular hypersurfaces are depicted in respective order in Fig. 9.
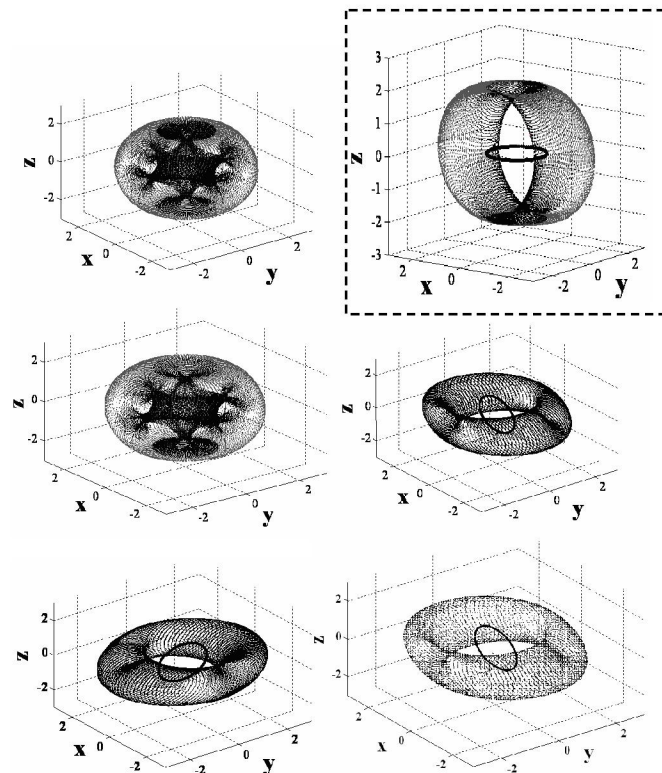

Fig. 9. Singular hypersurfaces resulting from 6 possible combinations of mixed skew angles. Singular surfaces from upper left correspond to sequence of mixed skew angles per Fig. 8.

Notice that three options for mixed skew angles result in the original momentum space rotated about $\hat{z}$ such that $\hat{x} \leftrightarrow \hat{y}$, while two other options generate spherical momentum space filled with significant internal singularities. Notice the center of the momentum space is clogged with singular surfaces such that those two figures are blackened in the center. Our difficulty seeing the center is indicative of difficulties steering a momentum vector through that space without striking a singular surface for those two mixed skew angle combinations.

One successful reorientation $\{\beta_1,\beta_2,\beta_3\}=\{90°,0°,90°\}$ is accomplished by simply sliding the second CMG from 90° to 0° resulting in yaw momentum maximization with the familiar internal singularity structure. Fig. 10 depicts a 3/4 CMG array skewed at mixed skew angles $\beta_1=90°$, $\beta_2=0°$, $\beta_3=90°$. CMG trajectories typically begin from zero momentum states and $\{\theta_1, \theta_2, \theta_3\}=\{0,0,0\}$ is obviously one such state. Trajectories originating at $\{\theta_1, \theta_2, \theta_3\}=\{0,0,0\}$ have 1H spherical momentum capability and *2H momentum capability about yaw ($\hat{z}$) singularity-free*. Momentum trajectories that are initiated from points near (0,0,2) can traverse to (0,0,-2) resulting in -4H being stored in the CMG array producing +4H momentum imparted to the spacecraft about yaw singularity free.
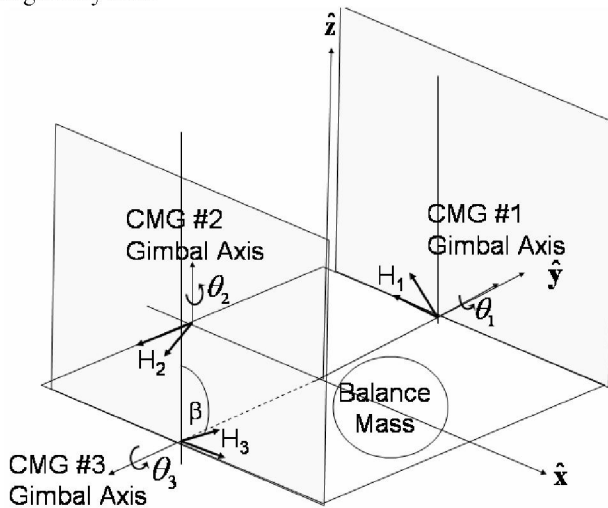

Fig. 10. $\{\beta_1,\beta_2,\beta_3\}=\{90°,0°,90°\}$ mixed skew angle momentum cutting planes depicted for a 3/4 CMG skewed array.

VII. EXPERIMENTAL VERIFICATION

Experimental verification is performed to demonstrate singularity free operations. A +5° degree yaw maneuver in 4 seconds is followed by a -5° yaw maneuver in 4 seconds. The attitude is then regulated to zero while the CMG continues to output significant torque to counter dramatic gravity gradient disturbances typical of imbalanced ground test spacecraft simulators. This maneuver has been previously performed using a skew angle of 57 degrees (not depicted). The CMG array became singular and attitude control was lost motivating this study. Skew angle was

increased to ninety degrees for all three CMGs, and the identical experiment was repeated. Notice in Fig. 11 that the maneuver is performed and the testbed is regulated for 5 minutes without striking any singular surfaces. Momentum magnitude and the inverse of the condition of the [A] matrix verify this assertion.

Notice what happens when the same momentum trajectory is placed in the context of the theoretical singular momentum space of the "optimal spherical" skew angle, $\beta=54.73°$ (Fig. 12). The internal singular surfaces are depicted individually for ease of visualization. This momentum trajectory is constantly close to the internal singular surfaces and quickly strikes a singular surface. A corresponding singular surface exists for a skew angle of 57°. Prior experiments using 57° went singular and resulted in the loss of attitude control when the momentum trajectory struck this corresponding singular surface.
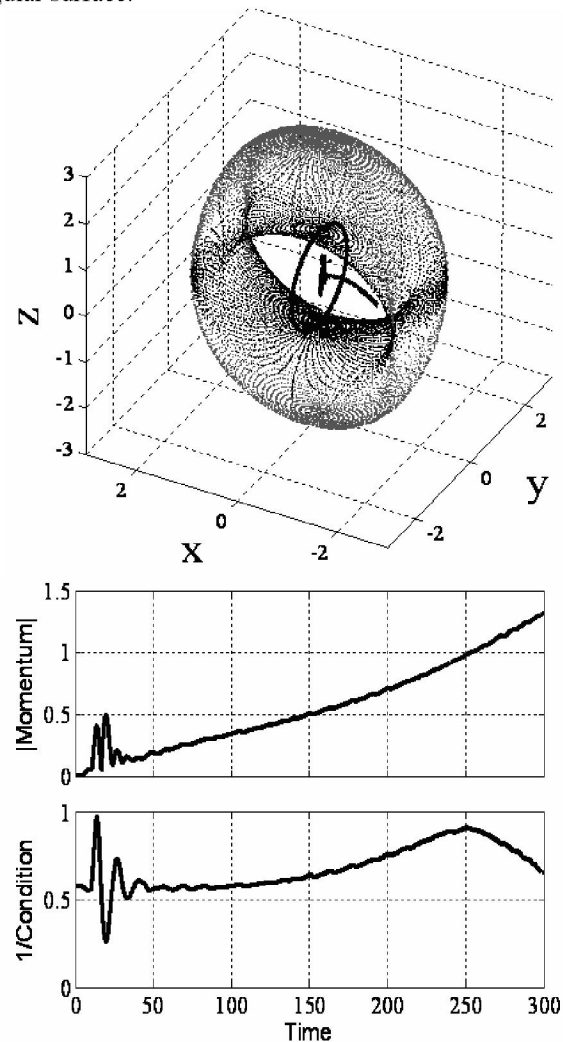

Fig. 11.   Experimental results: +5° yaw in 4 seconds, -5° yaw in 4 seconds, then regulate at $\{x,y,z\}=\{0,0,0\}$ countering cg-offset disturbance torque of unbalanced ground test satellite simulator. Momentum trajectory placed in context of theoretical singular momentum hypersurface of $\beta_i=90°$configuration. Magnitude of normalized momentum and inverse of condition number of [A] matrix (would approach zero if array became singular).

1555

Next, experiments were performed with mixed skew angles to orient the maximum momentum capability about the yaw axis as seen in Fig, 13 & Fig. 14. The maneuvers were increased 160% in the same duration from 5° to 13° in only 4 seconds. This demands significantly more momentum change specifically about yaw. The momentum is achieved singularity free and maneuver is performed without incident.
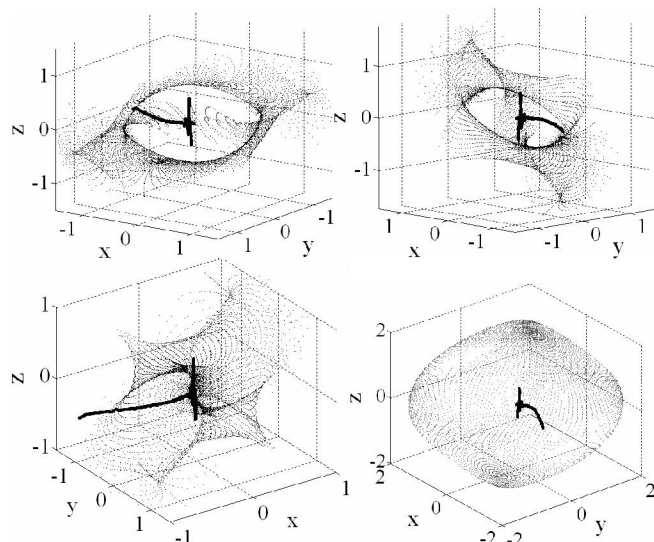

Fig. 12. Experiment from Fig. 11 performed in $\beta_i=90^\circ$ configuration placed in context of "optimal spherical" $\beta_i=54.73^\circ$ for the purpose of comparison (plots rotated for clarity). Note continuous flirting with singular surfaces and impact with surface occurs less than ¼ way through trajectory. This trajectory would not have continued as depicted had the skew angles been $\beta_i=54.73^\circ$. Instead the array would have gone singular and attitude control would have been lost.
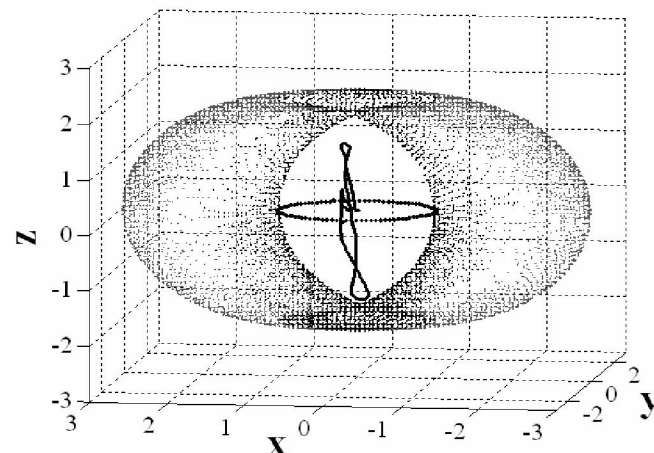

Fig, 13. Experimental results: $+13^\circ$ yaw in 4 seconds, -13° yaw in 4 seconds performed in $\{\beta_1,\beta_2,\beta_3\}=\{90^\circ,0^\circ,90^\circ\}$ mixed skew angle configuration. Momentum trajectory placed in context of theoretical singular hypersurface

VIII. CONCLUSION

This paper demonstrates a much desired goal of CMG attitude control, extremely high torque without mathematical singularity thus without loss of attitude control.
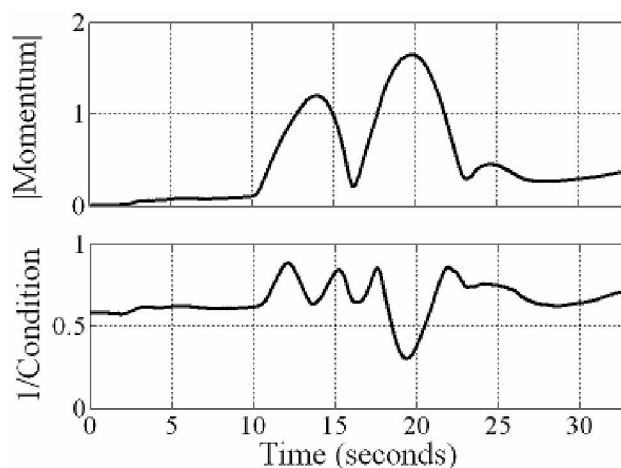

Fig. 14. Experimental results: $+13^\circ$ yaw in 4 seconds, -13° yaw in 4 seconds performed in $\{\beta_1,\beta_2,\beta_3\}=\{90^\circ,0^\circ,90^\circ\}$ mixed skew angle configuration. Maneuver momentum and inverse condition of [A].

The method is derived analytically and heuristically then experimentally verified. A 3/4 CMG array with mixed skew angles is capable of far superior performance than the commonplace 4 CMG pyramid skewed at 54.73°. It has the advantage of utilizing the same hardware geometry, thus attitude control engineers can duplicate these dramatic performance improvements simply by turning off one CMG and rotating the skew angles. With these alterations, no algorithm changes are required. As a matter of fact, the simple minimum $\|2\|$-norm pseudoinverse matrix inversion may be used without any kind of singularity-avoidance scheme within the bounds of the singularity-free momentum space.

REFERENCES

[1] Bong Wie, Space Vehicle Dynamics Control, pp. 439, AIAA, 98.
[2] J. Paradiso, "A Search-based approach to steering single-gimbaled CMGs", CSDL-R-2261, p. 17,26, 1991.
[3] D.J. Liska and Jacot Dean, "Control moment gyros", AIAA 2nd Annual Meeting Paper Preprint Number 65-405, July 1965.
[4] Haruhisa Kirokawa, "Geometric study of single gimbal control moment gyroscopes", Tech. Report Mech. Engin. Lab No. 175, June 7, 1997.
[5] G. Magulies and J.N. Aubrun, "Geometric theory of single-gimbal control moment gyro system", Journal of Astronautical Sciences, Vol. 26, No.2, pp. 159-191, 1978.
[6] N.S. Bedrossian, J. Paradiso, E.V. Bergmann, D. Rowell, "Steering law design for redundant single-gimbal control moment gyroscope", AIAA Journal of Guidance, Control, and Dynamics, Vol. 13, No. 6, pp. 1083-1089, 1990.
[7] S.R. Valadi, S. Krishnan, "Suboptimal command generation for control moment gyroscopes and feedback control of spacecraft", Proceedings of AIAA Guidance, Navigation, and Control Conference, pp. 637-646, Aug, 1994].
[8] D.E. Cornick, "Singularity avoidance control laws for single gimbal control moment gyros, Proceedings of AIAA Guidance and Control Conference 79-1968, pp. 20-33, 1979 (Martin Marietta Corp.).
[9] J. Paradiso, "Global steering of single gimbaled control moment gyroscopes using a directed search", AIAA Journal of Guidance, Control, and Dynamics, Vol. 15, No. 5, pp. 1236-1244, 1992.